ANALYSIS OF FLIGHT MECHANICS OF A NEW CIVIL SUPERSONIC AIRCRAFT CONCEPTUAL DESIGN

C. Christmann, F. Sachs
German Aerospace Center (DLR), Institute of Flight Systems,
Lilienthalplatz 7, 38108 Braunschweig, Germany

J. Kirz
German Aerospace Center (DLR), Institute of Aerodynamics and Flow Technology,
Lilienthalplatz 7, 38108 Braunschweig, Germany

Abstract

The DLR-project STORMIE investigates novel concepts for supersonic passenger transport, with a particular focus on low boom characteristics. Three aircraft designs are being developed and analyzed for this purpose. This paper presents a flight mechanics analysis of one of these aircraft designs – a supersonic business jet – conducted during the early stages of aircraft design within the DLR project STORMIE. Key characteristics of the investigated aircraft design are briefly presented, along with the workflow used to generate the configuration dataset, which is a prerequisite for the flight mechanics analysis. A six-degrees-of-freedom flight dynamics model, based on aerodynamic, propulsion, and mass properties data, is applied for the flight mechanics analysis. Furthermore, the software environment used for the flight performance analysis and the investigated flight conditions are described. A brief theoretical background on the flight mechanics requirements is outlined, and the results of the conducted analyses are presented and discussed. The flight mechanics analysis has shown that not all flight performance parameters yet meet the specified requirements. Furthermore, the aircraft's stability presents challenges in certain regions of the flight envelope, necessitating a review of the aircraft design.

Keywords

STORMIE, supersonic aircraft design, multi-fidelity, stability, flight mechanics

NOMENCLATURE

Abbreviations

CFD	Computational Fluid Dynamics
COAST	CPACS-Oriented Aircraft Simulation Tool
CPACS	Common Parametric Aircraft Configuration Schema
DLR	German Aerospace Center
FSTA	Future Supersonic Transport Airliner
FSTB-L	Future Supersonic Transport Business Jet Low-boom
LTO	Landing and Takeoff
MAC	Mean Aerodynamic Chord
RANS	Reynolds-Averaged Navier-Stokes
RCE	Remote Component Environment
SEP	Specific Excess Power
STORMIE	Supersonic Transport Open Research Models and Impact on Environment
TLAR	Top Level Aircraft Requirements
WGS	World Geodetic System
XML	Extensible Markup Language

List of symbols

C_L	Lift coefficient (-)
$C_{L\alpha}$	Lift coefficient gradient w.r.t. angle of attack (1/rad)
$C_{m\alpha}$	Pitching moment coefficient gradient w.r.t. angle of attack (1/rad)
c_{MAC}	Mean aerodynamic chord (m)
D	Drag (N)
FF	Fuel flow (kg/s)
g	Gravitational acceleration (m/s²)

doi: 10.25967/650245

h	Altitude (m)
h_e	Energy height (m)
K_n	Static margin (–)
P_s	Specific excess power (m/s)
P_{avail}	Available specific excess power (m/s)
P_{req}	Required specific excess power (m/s)
S	Wing area (m²)
T	Thrust (N)
V	Airspeed (m/s)
W	Weight (N)
x_{ac}	x-position of aerodynamic center (m)
x_{cg}	x-position of center of gravity (m)
α	Angle of attack (rad)

1. INTRODUCTION

Three major environmental challenges exist for civil supersonic transport: the LTO (landing and takeoff) noise primary from engines capable to accelerate the aircraft to supersonic speeds, the sonic boom, and increased emissions compared to subsonic aircraft. The STORMIE (Supersonic Transport Open Research Models and Impact on Environment) project was established at DLR (German Aerospace Center) in order to inform the discussion of certification standards for supersonic transport [1]. FIG 1 visualizes representative supersonic aircraft concept that are designed in STORMIE with the objective of assessing and minimizing their environmental impacts.

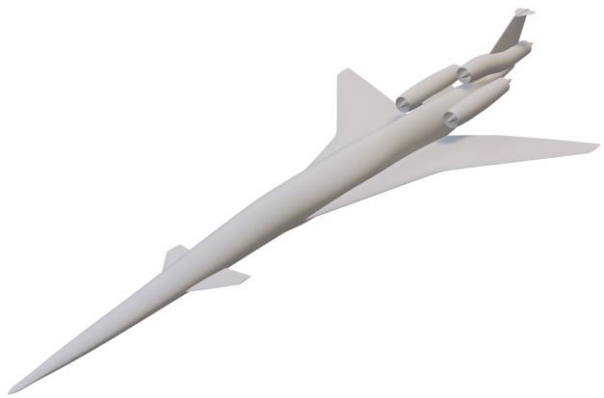

FIG 1. Renderings of the FSTB-L

However, before assessing the environmental impact, it is advisable to subject the aircraft to a preliminary flight mechanics analysis. This allows for the timely identification and mitigation of any deficiencies in stability, controllability, or flight performance.

The investigated aircraft configuration and the development of the configuration dataset are described in section 2. Section 3 briefly introduces the aircraft simulation framework used by the flight performance analysis tool, which is detailed in section 4. The flight mechanics analysis of selected parameters is also presented in section 4. Finally, section 5 provides the conclusions.

2. AIRCRAFT CONFIGURATION AND DATA SET

The STORMIE configurations' Top Level Aircraft Requirements (TLARs), detailed in TAB 1, are aligned with both market trends and technological advancements [2]. These requirements serve as the input for the preliminary design tool, OpenAD [3], which has been expanded to support supersonic civil aircraft design [4].

TLAR	Business Jet (FSTB-L)
Cruise Mach number	1.4
Passenger capacity	8
Range	4000 NM
Initial cruise altitude	> 45,000 ft
Entry into service	2030

TAB 1. Top level aircraft requirements for the STORMIE configurations

For the flight mechanics analysis presented later in this paper, the FSTB-L concept is used as an example, representing a business jet with three engines (FIG 2). Studies conducted during the early conceptual design phase of the project have shown that canard configurations offer significant potential for reducing sonic boom while enhancing aerodynamic efficiency, leading to the selection of the current design. Thus, the configuration was designed as a canard and T-tail concept.

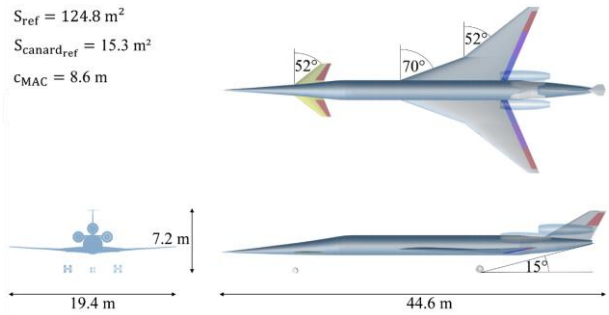

FIG 2. Three-view and dimensions of the FSTB-L [5]

In later stages of the project with more and more detailed analyses it turned out that achieving stability and controllability at all flight conditions is challenging, which was not foreseen in the initial design. The maximum takeoff mass (MTOM) resulting from the conceptual design is 47,400 kg.

The aircraft pitching motion is controlled by the canard and its integrated elevator. The canard functions as a horizontal stabilizer and is primarily used for trim, while the elevator, located at the rear of the canard, is used for active and rapid control inputs. During certain phases of flight, high demands are placed on canard response time, as the canard trim position must follow the pitch control input to support the pitch command. A very dynamic phase of flight is the aircraft rotation during takeoff. The T-tail at the rear of the aircraft does not contribute to pitch control. It is attached to the vertical tail in order to reduce the sonic boom loudness of the overall configuration. Roll control is achieved by the outer wing control surfaces on trailing edge of the delta wing. Yaw control is provided by the rudder mounted on the vertical stabilizer above the center engine.

The STORMIE project utilizes the CPACS (Common Parametric Aircraft Configuration Schema) [6] data definition for the air transportation system. It is an XML-based format that allows to exchange aircraft data between different disciplines in distributed processes. An exemplary workflow applied in STORMIE to obtain the CPACS dataset for the flight mechanical assessments is shown in FIG 3.

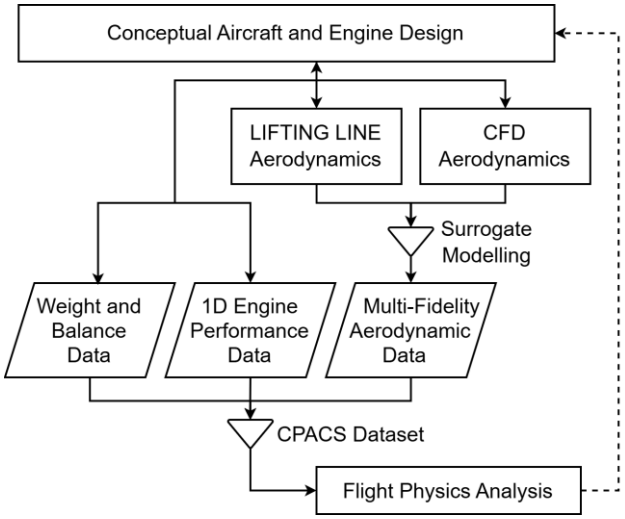

FIG 3. Workflow applied in STORMIE to enable flight mechanical assessments

The aerodynamic performance data is generated from a large quantity of low-fidelity LIFTING LINE simulation results (subsonic conditions) and a smaller quantity of higher-fidelity CFD simulation results (sub- and supersonic conditions at high altitudes). This data is mathematically combined to create multi-fidelity data tables. A detailed description of the process to obtain the multi-fidelity aerodynamic performance data based on surrogate models is provided by Schnell et. al. in Ref [5].

The engines for the STORMIE aircraft are designed using the DLR engine preliminary design platform GTlab [7]. An existing design process was applied with design requirements adapted to the respective airframe configurations. The dataset includes two different engine performance maps. The first engine performance map models the full flight envelope with thrust ranging from minimum to maximum, limited by total temperature at selected engine stations or low-pressure shaft speed. A second engine performance map was created especially for takeoff, whose data is limited to a flight speed of 250 knots below 10,000 ft in order to reflect the demands of derated takeoffs. As highlighted in the introduction, procedures in the terminal manoeuvring area, such as landing and takeoff, represent the second key area of interest for noise considerations. The typically high jet velocity at the engine nozzle of a supersonic jet aircraft is a major source of aircraft noise, even in low-speed flight conditions or on the ground. Therefore, the second engine performance map reflects the derated operation mode of the engine, ensuring that the exhaust gas velocity remains subsonic. The engine thrust itself is limited to a defined engine pressure ratio.

The conceptual design process directly yields weight and balance data, including aircraft masses, center of gravity, and moments of inertia for various defueling strategies.

3. AIRCRAFT SIMULATION FRAMEWORK

For the evaluation of aircraft flight performance, the 6-degrees-of-freedom (6DoF) fixed-wing aircraft simulation tool COAST (CPACS-Oriented Aircraft Simulation Tool) [8] was utilized. Implemented in MATLAB®/Simulink®, COAST is specifically tailored to the CPACS data structure and designed for use in multi-disciplinary optimization (MDO) toolchains. It comprises three main components: CPACS import functions (wrapper functions), a Simulink® simulation model, and postprocessing analysis code.

The wrapper functions import relevant aircraft data from CPACS, parsing XML data from structures like propulsion and aerodynamics and restructuring it for the simulation model. These functions leverage the MATLAB® interfaces of the open-source libraries TiXI [9] and TiGL [10].

The simulation model combines native Simulink® implementations for non-CPACS-specific components – such as the equations of motion, Earth model, and atmospheric model – with CPACS-specific components implemented as C++ S-functions. This approach, including the control chain, aerodynamics, and propulsion, provides greater flexibility and processing speed. Within the STORMIE project, COAST was extended with a CPACS-specific landing gear model [11] to enable performance and noise assessments during takeoff and landing. Currently, the equations of motion assume a rigid body, though future updates may incorporate flexible degrees of freedom, as supported by the CPACS standard.

COAST incorporates a flight control system (FCS) based on a nonlinear model-following control architecture and an integrated control allocation algorithm [8]. This algorithm automatically determines optimal control surface deflections based on surface effectiveness, allowing for closed-loop simulation across a wide range of aircraft configurations.

The third component of COAST provides postprocessing functions for trimming, linearization, and analysis of stability and control characteristics. Stability and control derivatives can be extracted for evaluating high-level stability and control indicators. Additionally, COAST offers output interfaces to other flight mechanics analysis tools, such as DLR's MAPET-FLT (for flight performance evaluation), which is described in section 4.

Thanks to its flexibility, COAST has been successfully applied to a diverse range of aircraft, including unmanned combat air vehicles, fighter aircraft [12], and supersonic civil aircraft (like the FSTB-L configuration investigated in this paper).

4. IN-FLIGHT PERFORMANCE EVALUATION

The purpose of this section is to give an overview of the in-flight performance of the FSTB-L aircraft at the end of the multi-disciplinary aircraft design process. A flight performance evaluation of an aircraft can be in general a very extensive process. On the one hand, to cover the complete flight dynamics it would be necessary to discuss and show a number of figures that would exceed scope of this paper. On the other hand, to give a significant characterization of an aircraft in terms of flight performance it is necessary to illustrate the essential points. Consequently, the analysis presented here is limited to selected parameters considered relevant to the design

process. This includes, for example, the expected flight envelope with achievable altitudes and airspeeds, or the assessment of stability during cruise flight.

Flight performance was evaluated using MAPET-FLT (Model-based Aircraft Performance Evaluation Tool – In-Flight Performance), a software tool developed within a MATLAB® environment. This current version builds upon the tool described in Ref. [13] and was enhanced to analyse both CPACS-based generic aircraft models and aircraft-specific flight dynamics models. This necessitated adapting MAPET-FLT to the aircraft simulation framework COAST, resulting in significant improvements and modifications. This section provides an overview of the FSTB-L aircraft's flight performance as part of the multi-disciplinary aircraft design process, offering initial insights into the flight characteristics of this low-boom supersonic concept. First, however, the functionality of the analysis tool will be examined in more detail.

4.1. Framework of In-Flight Performance Evaluation

The flight performance analysis within MAPET-FLT is structured into three main stages: preprocessing, solving, and postprocessing. The analyses are based on trim calculations for various steady flight conditions. These calculations are performed by a trim routine that determines aircraft states and control inputs to achieve equilibrium for forces and moments, considering only non-accelerated flight states. Within MAPET-FLT, these steady conditions are defined as "trim cases," categorised as either steady cruise or steady thrust.

In steady cruise, the aircraft is trimmed for unaccelerated horizontal level flight (flight path angle γ = 0°), with the trim function automatically determining the required power setting. In steady thrust, the trim problem is solved with a fixed engine thrust, resulting in a flight path angle γ between the steepest descent angle and the maximum achievable climb angle (or lowest descent angle if insufficient thrust is available). For each trim case, the total mass, altitude, and Mach number are varied, and the aircraft model is trimmed, yielding a unique trim point. Varying these parameters creates a trim matrix for each trim case, and the results from all trim points are stored for subsequent postprocessing and determination of flight performance parameters.

This final stage of the analysis process enables the evaluation of the aircraft's flight performance in various scenarios.

4.2. Investigated Flight Conditions

Reference [14] details concepts for landing and takeoff noise and CO_2 emission requirements for supersonic transport (SST) airplanes, including the definition of reference masses for Specific Air Range (SAR) measurements (cf. subsection 4.6). However, due to differences between subsonic and SST aircraft (e.g. high fuel fraction and flight performance characteristics of supersonic designs), an alternative approach is proposed. This approach selects high and low aircraft gross masses representative of initial and end-of-cruise conditions, based on the aircraft's design mission. For the FSTB-L, a high aircraft gross mass of 43,422 kg (84 % fuel) and a low aircraft gross mass of 27,418 kg (20 % fuel) were selected and employed in the estimation of relevant flight performance parameters.

For aerodynamics, the multi-fidelity aerodynamic performance map is used, which, as described earlier in subsection 2, was created from low-fidelity LIFTING LINE data and a smaller quantity of higher-fidelity CFD simulation results. Since the flight dynamics analysis is intended to cover the entire flight envelope, the general engine map is used as the data basis.

In order to meet the varying stability and control requirements associated with centre of gravity position [15], the project opted to define a fixed CG location for the initial analyses. As is known from previous supersonic designs, the shift in aerodynamic centre and centre of pressure at supersonic Mach numbers causes trim imbalances. Compensation for any imbalances is achieved through fuel pumping, analogous to the system used on the Concorde, utilizing a dedicated trim tank in the rear of the aircraft [16].

The following figure shows the centre of gravity range as a function of fuel mass. It illustrates both the maximum forward centre of gravity position and the maximum aft centre of gravity position that can occur depending on the fuel mass and distribution. It is important to note that the presented CG limits do not define the entire allowable CG envelope, as stability and controllability requirements have not yet been considered.

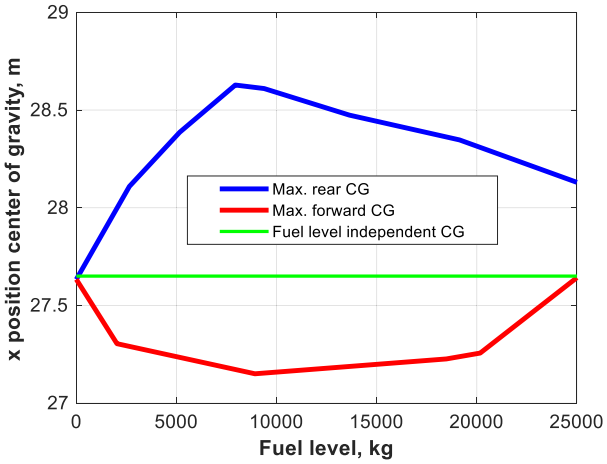

FIG 4. Center of gravity position at different fuel levels

The green line highlights the centre of gravity that can be theoretically maintained regardless of fuel loading. Consequently, a centre of gravity of 27.65 m was chosen for the flight performance analysis. Furthermore, this value reflects the centre of gravity position during takeoff, when the aircraft mass is at its maximum and the resulting forces for lift, propulsion, and trim are also maximal.

4.3. Estimation of Flight Envelope

Flight envelope estimation in MAPET-FLT is based on evaluating the trimmed aircraft at steady cruise conditions across a set of discrete trim points. The trim routine calculates the necessary thrust, angle of attack, and control inputs to achieve stable cruise for each trim point – defined by a unique combination of total mass, altitude, and Mach number. Therefore, the range of each trim matrix dimension must encompass the aircraft's estimated flight performance limits. The limits chosen for this analysis are given in TAB 2 below.

	Lower limit	Upper limit	Trim input dimensions
Total aircraft mass	27,418 kg	43,422 kg	2
Altitude	0 m	17,000 m	69
Mach number	0.2	1.6	141

TAB 2. Trim matrix range for flight performance evaluation

A high-resolution grid was employed to define the trim matrix to precisely represent the limits of the flight envelope. FIG 5 and FIG 6 each show the resulting trim points for steady cruise flight conditions for the two aircraft masses, and the estimated flight envelope.

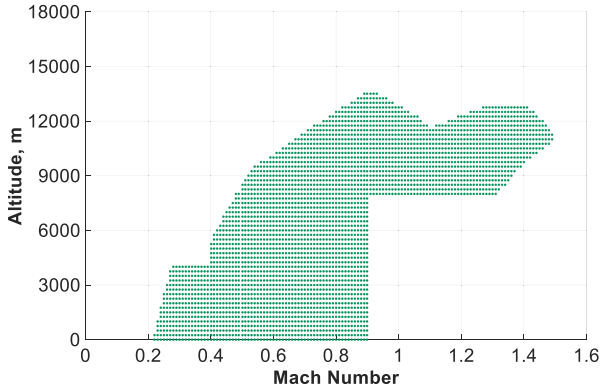

FIG 5. Estimated flight envelope for high aircraft gross mass (84 % fuel)

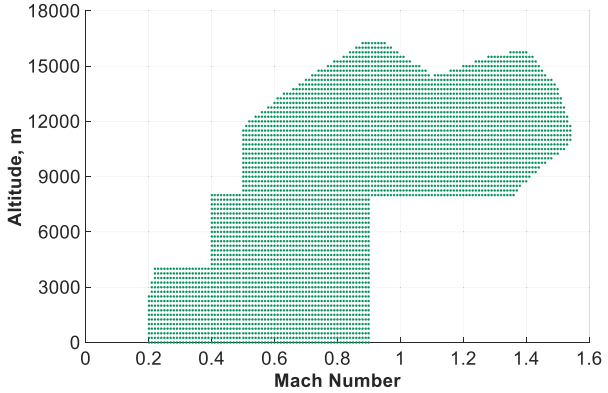

FIG 6. Estimated flight envelope for low aircraft gross mass (20 % fuel)

A data gap exists at Mach numbers above 0.9 and altitudes below 8,000 m due to a lack of corresponding aerodynamic data. The development of the aerodynamic performance map, including its challenges and limitations, is detailed in [5]. Although the aircraft is expected to be capable of flight within this region, the trim function flags these conditions as invalid due to insufficient aerodynamic data. Similar gaps are present at low speeds. Additional aerodynamic data is required to fully define the flight performance-driven speed limits. Nevertheless, the boundaries of the flight envelope can be seen from FIG 5 and FIG 6.

The flight envelope boundaries at high speed and altitude are limited by engine thrust. As shown in FIG 7, the example thrust curves for high aircraft gross mass indicate that the required thrust (blue curve) exceeds the available thrust (magenta curve) not only at the limits of the Mach number range. The regions of insufficient thrust are highlighted in red for clarity. Between 12,000 m and 13,000 m altitude, the required thrust surpasses the available thrust even at intermediate Mach numbers. Consequently, during the initial phase of cruise flight (at high gross mass) acceleration to supersonic speeds can only be achieved at altitudes below 12,000 m. As the cruise flight progresses, altitude can be increased up to 15,000 m. The reduction in available thrust around $Ma = 1.4$ is due to reaching the maximum permissible compressor temperature (T3).

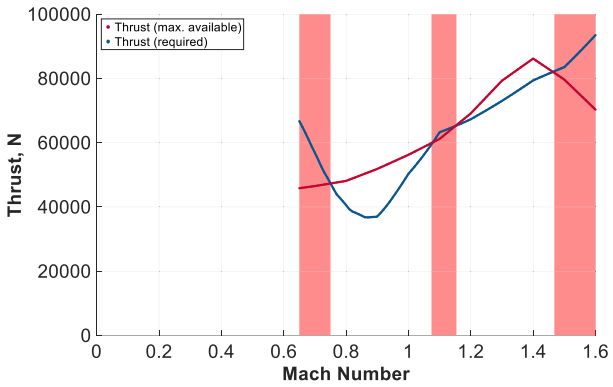

FIG 7. Thrust curve for high gross mass (84 % fuel) at 12,000 m

It is also apparent that the lowest thrust requirement occurs in the high subsonic regime, approximately at Mach 0.9. Despite these deficiencies, it is evident that the target cruise Mach number of $Ma = 1.4$ is readily achieved, and the TLAR is therefore satisfied.

4.4. Estimation of Service Ceiling

The service ceiling is the maximum altitude an aircraft can reach during normal operations while maintaining a climb rate above a specified value. While a climb rate of 100 feet per minute (0.5 m/s) is commonly reported in the literature, certain references [17–19] indicate higher values for civil transport aircraft, for example, 500 feet per minute (2.5 m/s) for jet aircraft. This value will also be employed in the subsequent analysis.

Specific Excess Power (SEP) is a crucial metric in flight performance analysis, particularly when evaluating manoeuvrability. It represents the amount of power available above what is required to maintain a specific flight condition (like straight and level flight). Essentially, it's the additional power an aircraft has to perform manoeuvres. Because of the following relationship:

$$P_s = \frac{P_{avail} - P_{req}}{W} = \frac{(T - D)V}{W} = \frac{dh}{dt} + \frac{V}{g}\frac{dV}{dt} \quad (1)$$

the climb rate is directly related to specific excess power. This relationship accurately reflects the rate of climb only when velocity V remains constant. For service ceiling estimation, MAPET-FLT offers a contour plot that shows

specific excess power (2.5 m/s) plotted against altitude and Mach number. The following figure FIG 8 shows the estimated service ceiling altitudes for the two defined aircraft gross masses.

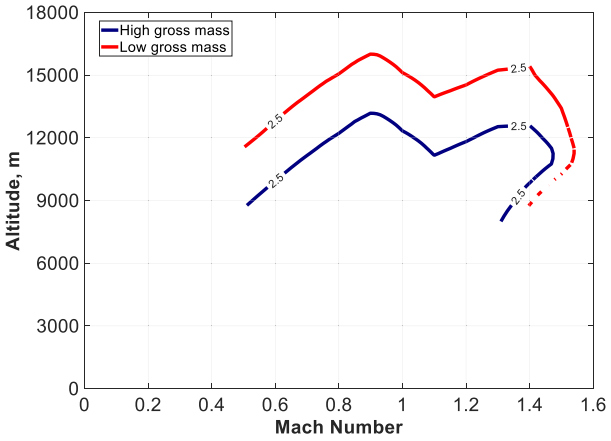

FIG 8. Estimated service ceiling for both aircraft gross masses

The TLAR specify a minimum initial cruise altitude of 45,000 ft (13,716 m). As can be seen from FIG 8, the heavy aircraft cannot reach the specified initial altitude at any Mach number. While the service ceiling is near the specified altitude at approximately $Ma = 0.9$ in the subsonic regime, it decreases to a maximum altitude of only approximately 12,000 m at the target cruise $Ma = 1.4$.

Considering the service ceiling of the lighter aircraft at the end of cruise, this is approximately 15,000 m at the aforementioned Mach numbers. Therefore, it is theoretically possible to climb to the initial cruise altitude or higher during the course of the flight.

4.5. Estimation of Static Margin

The static margin (K_n) is a measure of an aircraft's static stability. It represents the allowable aft movement of the center of gravity before longitudinal static instability occurs, and is equivalent to the distance between the center of gravity (x_{cg}) and the aerodynamic center (x_{ac}). The static margin is directly proportional to the pitching moment coefficient derivative, $C_{m\alpha}$. The static margin is defined by the following equation [17 p. 217]:

$$K_n = \frac{x_{cg} - x_{ac}}{c_{mac}} = -\frac{C_{m\alpha}}{C_{L\alpha}} \tag{2}$$

As the aerodynamic center coincides with the neutral point, the static margin can also be defined as the distance between the center of gravity and the neutral point. For static stability, this margin must be positive, indicating that the center of gravity is located forward of the neutral point and that the pitching moment coefficient decreases with increasing angle of attack. In this context, the static margin is normalized by the mean aerodynamic chord. The figure below shows the static margin's variation with Mach number at an altitude of 10,000 m as a representative example. Trends at higher altitudes are only slightly different and are therefore omitted for clarity.

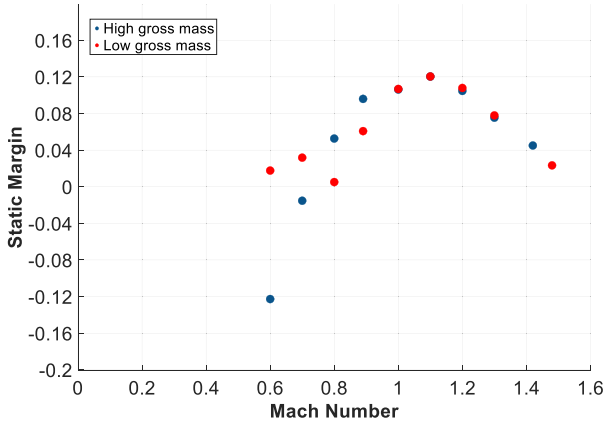

FIG 9. Estimated static margin over Mach number at 10,000 m for both gross masses

Figures FIG 9 clearly show the increase and subsequent decrease in the stability margin at higher Mach numbers. This is caused by the rearward shift of the neutral point, and thus the increasing distance from the center of gravity as the aircraft traverses the sound barrier, which is consistent with expectations.

Within the higher Mach number range, the stability margin of the aircraft remains positive for both aircraft masses, indicating that the center of gravity is located forward of the neutral point and the aircraft is statically stable. However, at the target cruise Mach number of $Ma = 1.4$, the stability margin is only 0.02-0.04, which, corresponds to a distance of only 17-34 cm between the center of gravity and the neutral point – a rather small margin.

Brockhaus et al. [20] presents flight mechanics data for selected flight conditions of the Concorde, which can be used to calculate the static margin for comparison:

	Altitude	Mach number	K_n
Approach	600 m	0.251	0.0129
Subsonic cruise	9,000 m	0.882	0.0223
Supersonic cruise	15,500 m	2.07	0.0547

TAB 3. Static margin for selected flight conditions for Concorde aircraft

For the Concorde, the static margin is even lower than that of the supersonic business jet under consideration. It is therefore possible to safely operate aircraft with such a low static margin. With a $c_{mac} = 27.5\ m$, these static margins correspond to a distance of 35-150 cm between the center of gravity and the neutral point.

For low Mach numbers the FSTB-L faces a negative static margin. This is undesirable and requires constructive or other technical counter measures, such as variable fuel distribution during flight. The aircraft's stability requirements (statically stable) are not met across the entire flight envelope, at least with respect to the scrutinised centre of gravity location.

4.6. Estimation of Specific Air Range

Today, aircraft are required to comply with CO_2 emission certification requirements, and evaluating these emissions is crucial for a fuel-efficiency analysis. The CO_2 emissions evaluation metric value in kg/km is determined during the certification or validation of an aircraft. It is a specific air range (SAR)-based metric adjusted by a dimensionless Reference Geometric Factor (RGF). The SAR is the distance an aircraft travels per unit of fuel consumed, typically expressed in meters per kilogram of fuel. The RGF is the external planform area of the pressurized cabin, excluding the cockpit, divided by 1 m² to form a dimensionless factor. The CO_2 metric value aims at measuring the technology (structural, propulsion, aerodynamic) performance of an aircraft type with respect to its fuel efficiency. Certification requirements for subsonic aircraft are detailed in Ref. [21]; however, adaptations were deemed necessary for supersonic transport aircraft [14].

The next generation of SST aircraft is expected to cruise supersonically over water and subsonically over land to mitigate the impact of sonic booms on populated areas. Consequently, specific air range estimation was conducted for transonic and supersonic Mach numbers at the aircraft masses defined in subsection 4.2. The RGF is not taken into account in the analysis at this stage.

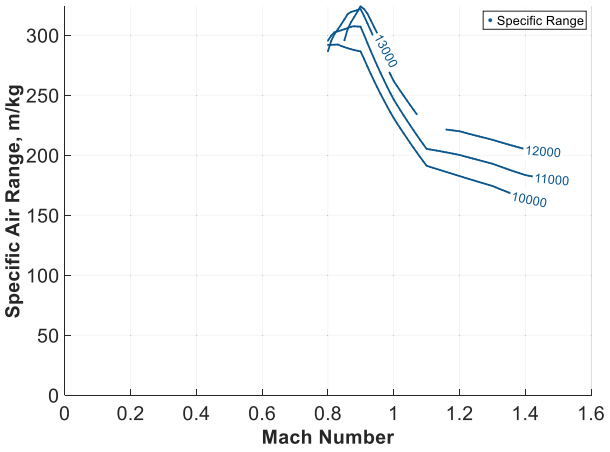

FIG 10. Estimated specific air range for high gross aircraft mass (84 % fuel)

The specific air range for the heavy aircraft shown in FIG 10 is approximately 300 m/kg in the high subsonic regime, decreasing to a range of 150-200 m/kg at the cruise Mach number of $Ma = 1.4$.

Towards the end of the cruise flight, the specific range is as expected greater, as the aircraft is now lighter and consequently consumes less fuel. Further increases can be achieved through a higher altitude. The maximum values presented in FIG 11 are approximately 500 m/kg in the high subsonic regime and around 300 m/kg during supersonic cruise.

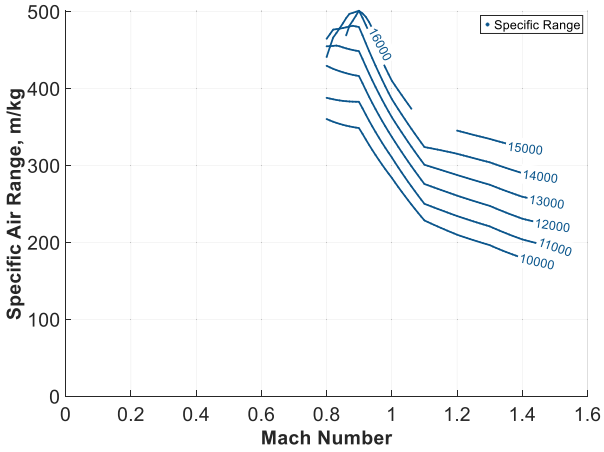

FIG 11. Estimated specific air range for low gross aircraft mass (20 % fuel)

As there is no comparable aircraft currently on the market, no benchmark values can be drawn at this point. A current business jet with comparable range, payload, and fuel loading (20 % fuel) exhibits a specific range of approximately 700-900 m/kg with maximum cruise thrust [22].

4.7. Estimation of Minimum Fuel Climb Schedule

A fuel-efficient flight is essential in civil aviation. In addition to fuel-optimal altitude and Mach number during cruise, an appropriate climb profile is also relevant. This is achieved using the so-called energy height method.

The minimum fuel climbing procedure is defined by the locus of all the tangent points of the constant specific energy lines and the constant specific excess power divided by fuel flow (SEP/FF) lines.

Specific excess power is calculated as described in subsection 4.4, but is represented with high resolution across the entire flight envelope. Fuel flow can be determined from the trim calculations. Specific energy is calculated using the following formula [17 p. 164] :

$$h_e = h + \frac{V^2}{2g} \tag{3}$$

The following figure FIG 12 shows constant specific energy lines (colored curves) and SEP/FF (blue lines) with maximum available thrust as a function of altitude and Mach number. The red line approximately connects the tangential intersection points of the constant SEP/FF lines with the constant specific energy lines. Acceleration to supersonic speeds has not been considered at this point.

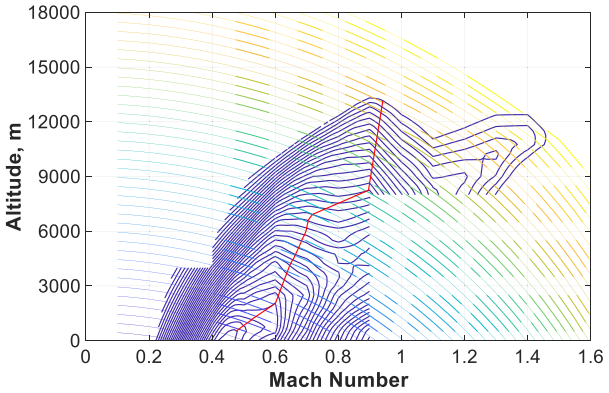

FIG 12. Estimation of minimum fuel climb schedule with SEP/FF (blue lines) and specific energy (colored lines)

Following the red line during climb minimizes fuel consumption. Further optimization of the line's trajectory, incorporating operational aspects, is necessary in the subsequent development process.

5. CONCLUSIONS

The STORMIE project aims to develop three supersonic aircraft configurations, which will be made publicly available. This paper focuses on flight mechanics analysis conducted on the FSTB-L; a supersonic business jet designed for low boom performance. A framework for flight mechanics simulations based on CPACS aircraft data is introduced, and results from trim calculations constitute the basis for flight mechanics analyses. These trim calculations were performed for both a light and a heavy aircraft.

Estimating the flight envelope revealed that the initial cruise altitude specified in the TLARs is undershot by roughly 5%. The initial top of climb will be reached with a lower fuel mass later in the flight. Simultaneously, a reduction in achievable altitude is observed after exceeding Mach 1, which can be attributed to a significant increase in thrust demand. This necessitates accelerating to supersonic cruise speed at a lower altitude, followed by a climb to a higher altitude. The cruise Mach number defined in the TLARs is readily achieved.

However, white areas are also visible in the flight envelope diagram, for which no aerodynamic data are available. During the creation of the aero performance maps, prioritizing coverage of a potential flight profile was paramount. To estimate the complete, flight-performance-based flight envelope, the maps should also have a corresponding extent.

Civil aircraft must be designed to be statically stable, meaning that the center of gravity must be located forward of the neutral point, resulting in a positive stability margin. Investigation at a representative altitude has shown that this is the case at higher Mach numbers, although over a wide range, the margin is only minimal. This circumstance requires a re-evaluation of the center of gravity location in flight as well as during landing and takeoff.

Specific range is a key parameter in assessing relevant emissions. As expected, this is significantly lower than that of current subsonic business jets. As the exact certification standards for supersonic aircraft have not yet been established, an assessment can only be performed at a later stage.

Finally, it was investigated how the aircraft can climb to cruise altitude in a fuel-efficient manner.

These findings will now be fed back into the development process and can also be considered in the analysis of the two other aircraft configurations that are still pending within the project.

References

[1] KIRZ, Jochen, BARTELS, Susanne, BERTSCH, Lothar, CAN, Ahmet Günay, DIETL, Tobias, EWERT, Roland, GRÄBERT, Matti, JARON, Robert, LIEBHARDT, Bernd, NÖDING, Michel, PLOHR, Martin, and SCHNELL, Samuel. Predicting Take-Off Noise, Sonic Boom, and Landing Noise of Supersonic Transport Aircraft Concepts [online]. *INTER-NOISE and NOISE-CON Congress and Conference Proceedings*. 2023. **268(**1), pp. 7288-7297. DOI: 10.3397/IN_2023_1096.

[2] WEBER, Lukas, BERTRAM, Pascal, DIETL, Tobias, SCHNELL, Samuel, PLOHR, Martin, and LIEBHARDT, Bernd. *Conceptual Design of Supersonic Transport Configurations. AIAA AVIATION Forum and ASCEND 2025*. DOI: 10.2514/6.2025-3263.

[3] WÖHLER, Sebastian, ATANASOV, Georgi, SILBERHORN, Daniel, FRÖHLER, Benjamin, and ZILL, Thomas. *Preliminary Aircraft Design within a Multidisciplinary and Multifidelity Design Environment. Aerospace Europe Conference 2020:* Council of European Aerospace Societies, 2020.

[4] DIETL, Tobias, SCHNELL, Samuel, SHIVA PRAKASHA, Prajwal, NAGEL, Björn, and BRODERSEN, Olaf. *Development of a Conceptual Design Tool for Supersonic Transport with a Variable Fidelity Interface* [online]. Bonn: Deutsche Gesellschaft für Luft- und Raumfahrt - Lilienthal-Oberth e.V. DOI: 10.25967/570137.

[5] SCHNELL, Samuel, TIDOW, Alexander, and KIRZ, Jochen. *Multi-Fidelity Aerodynamic Data Set Generation and Analysis of the FSTB-L Supersonic Business Jet. AIAA AVIATION Forum and ASCEND 2025*. DOI: 10.2514/6.2025-3264.

[6] Deutsches Zentrum für Luft- und Raumfahrt e.V. German Aerospace Center (DLR). *CPACS* [online]. *A Common Language for Aircraft Design*. https:/www.cpacs.de.

[7] REITENBACH, Stanislaus, VIEWEG, Maximilian, BECKER, Richard, HOLLMANN, Carsten, WOLTERS, Florian, SCHMEINK, Jens, OTTEN, Tom, and SIGGEL, Martin. *Collaborative Aircraft Engine Preliminary Design using a Virtual Engine Platform, Part A: Architecture and Methodology. AIAA SciTech 2020 Forum*. DOI: 10.2514/6.2020-0867.

[8] KIEHN, Daniel, AUTENRIEB, Johannes, and FEZANS, Nicolas. *COAST - A Simulation and Control Framework to Support Multidisciplinary Optimization and Aircraft Design with CPACS. 33rd Congress of the International Council of the Aeronautical Sciences:* International Council of the Aeronautical Sciences (ICAS), 04-09 September 2022.

[9] Deutsches Zentrum für Luft- und Raumfahrt e.V. German Aerospace Center (DLR) (DLR). *GitHub - DLR-SC/tixi: A simple XML interface library* [online]. https://github.com/DLR-SC/tixi.

[10] Deutsches Zentrum für Luft- und Raumfahrt e.V. German Aerospace Center (DLR). *The TiGL Geometry Library* [online]. https://dlr-sc.github.io/tigl/.

[11] HÄHNEL, Robin. *Modellbildung, Implementierung und Simulation eines parametrisierbaren Fahrwerkmodells für ein Überschallverkehrsflugzeug.* Masterarbeit. TH Wildau, 2024.

[12] CHRISTMANN, Carsten, KIEHN, Daniel, STRADTNER, Mario, and LIERSCH, Carsten M. *Initial Assessment of Stability and Controllability in the Early Stage of Combat Aircraft Design* [online]. 2023. Bonn: Deutsche Gesellschaft für Luft- und Raumfahrt - Lilienthal-Oberth e.V. DOI: 10.25967/570283. urn:nbn:de:101:1-202301061427231248485l.

[13] OHME, Per, and RAAB, Christian. *A Model-Based Approach to Aircraft Performance Assessment. AIAA Atmospheric Flight Mechanics Conference and Exhibit*. DOI: 10.2514/6.2008-6873.

[14] European Union Aviation Safety Agency (EASA). *Environmental protection requirements for supersonic transport aeroplanes. A-NPA 2022-05,* 22-MAY-2022.

[15] SACHS, Falk, CHRISTMANN, Carsten, SCHNELL, Samuel, KIEHN, Daniel, and HÄHNEL, Robin. *Flight Physics Analysis for the FSTB-L Supersonic Business Jet. AIAA AVIATION Forum and ASCEND 2025*. DOI: 10.2514/6.2025-3265.

[16] EAMES, John D. *Concorde Operations. SAE Technical Paper Series.* Warrendale, PA, United States: SAE International, 1991. DOI: 10.4271/912161.

[17] HULL, David G. *Fundamentals of airplane flight mechanics. With 25 tables*. Berlin, Heidelberg: Springer, 2007. ISBN 3-540-46571-5.

[18] SCHEIDERER, Joachim. *Angewandte Flugleistung. Eine Einführung in die operationelle Flugleistung vom Start bis zur Landung.* Berlin, Heidelberg: Springer, 2008. ISBN 978-3-540-72724-8.

[19] MARCHMAN III, James F. *Aerodynamics and Aircraft Performance.* 3rd edition. Minneapolis, MN: Virginia Tech Libraries, 2004. Open textbook library. ISBN 978-1-949373-63-9.

[20] BROCKHAUS, Rudolf, ALLES, Wolfgang, and LUCKNER, Robert. *Flugregelung.* 3., neu bearb. Aufl. Berlin, Heidelberg: Springer, 2011. DOI: 10.1007/978-3-642-01443-7. ISBN 978-3-642-01443-7.

[21] International Civil Aviation Organization (ICAO). AN16-3. First Edition. *Annex 16: Environmental Protection. Volume III - Aeroplane CO2 Emissions First Edition, July 2017.* Montreal: ICAO.

[22] Dassault Aviation. *FALCON 2000EX EASy, FALCON 2000DX, FALCON 2000LX* [online]. *Airplane Flight Manual.* DGT88898 [viewed 25 August 2025]. https://downloads.regulations.gov/FAA-2013-0862-0005/attachment_1.pdf.